

The Role of Evolutionary Age and Metallicity in the Formation of Classical Be Circumstellar Disks I. New Candidate Be Stars in the LMC, SMC, and Milky Way

J.P. Wisniewski^{1,3} & K.S. Bjorkman^{2,3}

ABSTRACT

We present B, V, R, and H α photometry of 8 clusters in the Small Magellanic Cloud, 5 in the Large Magellanic Cloud, and 3 Galactic clusters, and use 2 color diagrams (2-CDs) to identify candidate Be star populations in these clusters. We find evidence that the Be phenomenon is enhanced in low metallicity environments, based on the observed fractional early-type candidate Be star content of clusters of age 10-25 Myr. Numerous candidate Be stars of spectral types B0 to B5 were identified in clusters of age 5-8 Myr, challenging the suggestion of Fabregat & Torrejon (2000) that classical Be stars should only be found in clusters at least 10 Myr old. These results suggest that a significant number of B-type stars must emerge onto the zero-age-main-sequence as rapid rotators. We also detect an enhancement in the fractional content of early-type candidate Be stars in clusters of age 10-25 Myr, suggesting that the Be phenomenon does become more prevalent with evolutionary age. We briefly discuss the mechanisms which might contribute to such an evolutionary effect. A discussion of the limitations of utilizing the 2-CD technique to investigate the role evolutionary age and/or metallicity play in the development of the Be phenomenon is offered, and we provide evidence that other B-type objects of very different nature, such as candidate Herbig Ae/Be stars may contaminate the claimed detections of “Be stars” via 2-CDs.

Subject headings: Magellanic Clouds — stars: emission-line, Be — circumstellar matter — techniques: photometric — clusters:individual (Bruck 60, Bruck 107, HW 43, NGC 371, NGC 456, NGC 458, NGC 460, NGC 465, LH 72, NGC 1850, NGC 1858, NGC 1955, NGC 2027, NGC 2186, NGC 2383, NGC 2439)

¹Universities Space Research Association/NASA GSFC Code 667, Building 21, Greenbelt, MD 20771, jwisnie@milkyway.gsfc.nasa.gov

²Ritter Observatory, Department of Physics and Astronomy MS 113, University of Toledo, Toledo, OH 43606, karen@physics.utoledo.edu

³Visiting Astronomer, Cerro Tololo Inter-American Observatory

1. Introduction

Classical Be stars are rapidly rotating, near main sequence B-type stars which show or have shown hydrogen Balmer emission (Jaschek et al. 1981). It is widely accepted that Be stars have gaseous, geometrically thin circumstellar disks (for a review, see Porter & Rivinius 2003). As summarized in Porter & Rivinius (2003), numerous mechanisms have been proposed to explain how circumstellar disks may form around classical Be stars, including the wind-compressed disk (WCD) model (Bjorkman & Cassinelli 1993), the magnetically torqued wind-compressed disk model (Cassinelli et al. 2002), and processes related to non-radial pulsations of the stellar photosphere (Rivinius et al. 2001), yet none have been completely successful in explaining the observed phenomena. Beginning with the work of Struve (1931), it has often been speculated that the fundamental source of the Be phenomenon is tied to the rapid rotation of these stars: the canonical assertion is that classical Be stars rotate at $v_{eq}/v_{crit} \sim 70\text{-}80\%$ of their critical velocity (Porter 1996; Porter & Rivinius 2003). However, recent theoretical work incorporating the effects of equatorial gravity darkening into studies of rotation rates (Townsend et al. 2004) suggests there is a degeneracy in the measurement of rotation rates such that increasing v_{eq} from 80% to 100% of the critical velocity has no effect on observed line widths. Thus classical Be stars may actually be rotating at or near their critical breakup velocity. Alternatively, Cranmer (2005) suggest that a subset of classical Be stars might be rotating at sub-critical rates as low as $0.4\text{-}0.6 v_{crit}$.

Studying stars from the Bright Star Catalog (Hoffleit & Jaschek 1982) and its supplement (Hoffleit, Saladyga, & Wlasuk 1983), Zorec & Briot (1997) found that the mean frequency of Be stars with respect to normal B stars was $\sim 17\%$ in the Galaxy. Zorec & Briot (1997) also found that the peak frequency occurred for spectral type B1, where 34% of B stars were Be stars, and noted no difference in frequencies between giant, dwarf, and subgiant type B stars. It should be noted however that the reliability of Bright Star Catalog spectral types is often questionable. Early studies also concluded that Galactic Be stars were present from the zero-age-main-sequence to the terminal-age main sequence (Mermilliod 1982; Slettebak 1985). Due in part to the advent of CCDs, systematic studies of the Be populations of star clusters and associations have expanded past our Galaxy to include the Magellanic Clouds (Feast 1972; Grebel, Richtler, & de Boer 1992; Grebel 1997; Dieball & Grebel 1998; Keller et al. 1999; Grebel & Chu 2000; Keller et al. 2000; Olsen et al. 2001). These extragalactic survey programs have typically used 2-color diagram (2-CDs) photometric techniques to identify the frequency of B-type stars exhibiting excess $H\alpha$ emission (“Be stars”) relative to normal B-type stars in stellar associations and clusters. General trends in the fractional Be content of a cluster as a function of its age and/or metallicity have been observed, leading to suggestions that secondary mechanisms, besides rapid rotation, might influence the development of Be circumstellar disks.

Mermilliod (1982); Grebel (1997); Fabregat & Torrejon (2000) and Keller (2004) have found that the frequency of the Be phenomenon seems to peak in clusters with a main sequence turn-off of B1-B2, leading to the suggestion that the Be phenomenon is related to a star’s evolutionary age. Fabregat & Torrejon (2000) suggested the Be phenomenon will start to develop only in the second half of a B star’s main sequence lifetime, owing to structural changes in the star. Specifically, Fabregat & Torrejon (2000) noted that Be star-disk systems should start to appear in clusters 10 Myr old, corresponding to the mid-point main sequence lifetime of B0 stars (Zorec & Briot 1997), and their frequency should peak in clusters 13-25 Myr old, corresponding to the mid-point main sequence lifetime of B1-B2 stars (Zorec & Briot 1997). Curiously, Keller et al. (1999) claimed to detect numerous Be stars in the Small Magellanic Cloud (SMC) cluster NGC 346, which has an age between 2.6 Myr (Kudritzki et al. 1989) and 5 Myr (Massey, Parker, & Garmany 1989); this result seems to conflict with Fabregat & Torrejon’s assertion. Hillenbrand et al. (1993) also suggested that numerous classical Be stars might be present in the young cluster NGC 6611; however, it is possible that these objects are pre-main-sequence Herbig Ae/Be stars (Fabregat & Torrejon 2000). Numerous mechanisms have been proposed to explain this apparent evolutionary effect, including structural changes within the central star (Fabregat & Torrejon 2000), an evolutionary spin-up of the central star (Meynet & Maeder 2000; Keller 2004), and spin-up due to mass-transfer in binary systems (McSwain & Gies 2005b).

Several photometric studies (Grebel, Richtler, & de Boer 1992; Mazzali et al. 1996; Grebel 1997; Maeder, Grebel, & Mermilliod 1999; Keller 2004) have suggested that the Be phenomenon may be more prevalent in low metallicity environments, based on comparisons of the apparent fractional Be populations of Galactic, Large Magellanic Cloud (LMC), and SMC clusters. IUE, HST, and FUSE observations (Garmany & Conti 1985; Bianchi et al. 1996; Fullerton et al. 2000) show that stars tend to have lower wind velocities in metal poor environments. The WCD model (Bjorkman & Cassinelli 1993) suggests that reducing terminal wind velocities would increase the likelihood that a B star experiencing mass-loss would be able to retain this matter in the form of a circumstellar disk, although Owocki, Cranmer, & Gayley (1996) claim non-radial line forces may inhibit such a scenario. Maeder (1999) suggests that the increase in the frequency of Be stars in low metallicity environments is related to the presence of a greater number of rapidly rotating stars in these locations, owing to a reduced coupling of the magnetic field and the young stellar object (Maeder, Grebel, & Mermilliod 1999; see also Penny et al. 2004).

The accuracy of these initial interpretations is hampered by numerous factors. Fabregat & Torrejon (2000) note that the photometric surveys used by many to identify Be stars only detect Be stars with high levels of emission, and likely miss weak emitters. Furthermore, since Be stars are known variables which can experience active and quiescent stages (Telting 2000;

Bjorkman et al. 2002), it is likely that some Be stars in a cluster might be in a quiescent stage and hence not identified as Be stars by these techniques. This possibility has been demonstrated by various followup investigations (Hummel et al. 1999; Keller et al. 1999), which do not detect 100% of previously identified Be stars in certain clusters; additionally, a significant number of previously unidentified Be stars are uncovered in these studies. Keller et al. (2000) note some spurious detections in photometrically identified Be stars located in crowded cluster cores. Even some spectroscopically identified Be stars (Mazzali et al. 1996) have been shown to be spurious detections caused by the presence of diffuse background H α emission (Keller & Bessell 1998). The number of clusters with accurately determined Be frequencies is still limited, especially regarding SMC clusters, thus small number statistics become important when attempting to draw broad conclusions from the literature data set.

In this paper, we provide a significant increase in the number of extragalactic clusters whose candidate Be populations have been identified photometrically. In section 2, we outline our observations and data reduction techniques. In section 3, we detail our identification of candidate Be stars in 8 SMC, 5 LMC, and 3 Galactic clusters. We offer a detailed discussion of how these results may shed insight into the role age and/or metallicity play in the development of the Be phenomenon in Section 4.

2. Observations and Data Reduction

Our photometry was obtained at the Cerro Tololo Inter-American Observatory (CTIO)¹ 0.9 m telescope using the direct imaging CCD, a 2048 x 2046 multi-amplifier CCD, operated in the quad amplifier mode. With the f/13.5 secondary, we recorded data over a field of view of 13'.5 x 13'.5 with a pixel scale of 0''.396 pixel⁻¹. We used CTIO's standard 3'' x 3'' B ($\lambda_{center} = 4201\text{\AA}$, $\delta\lambda = 1050\text{\AA}$), V ($\lambda_{center} = 5475\text{\AA}$, $\delta\lambda = 1000\text{\AA}$), R ($\lambda_{center} = 6425\text{\AA}$, $\delta\lambda = 1500\text{\AA}$), and H α ($\lambda_{center} = 6563\text{\AA}$, $\delta\lambda = 75\text{\AA}$) filters. A summary of our observations along with relevant cluster information is given in Table 1. Overscan correction, image trimming, bias correction, and flat fielding of the data were achieved using standard IRAF² techniques.

To calibrate to the standard B,V,R system, we obtained photometry of 3-4 standard fields, identified by Landolt (1992), per night. The observations were not made under photometric conditions. Aperture photometry was performed for all standard stars using an

¹The Cerro Tololo Inter-American Observatory is operated by the Association of Universities for Research in Astronomy, under contract with the National Science Foundation.

²IRAF is distributed by the National Optical Astronomy Observatories, which are operated by the Association of Universities for Research in Astronomy, Inc., under contract with the National Science Foundation.

aperture radius of 12 pixels. Transformations were derived from least-squares fits to the following equations

$$\begin{aligned} m_b &= B_0 + (B_1 * X_b) + (B_2 * (B - V)) \\ m_v &= V_0 + (V_1 * X_v) + (V_2 * (B - V)) \\ m_r &= R_0 + (R_1 * X_r) + (R_2 * (V - R)), \end{aligned}$$

where X is the airmass and the lowercase letters indicate instrumental magnitudes in each filter. The transformation coefficients for each night are given in Table 2. Given our limited number of observations of standard fields, we found it necessary to hold the the coefficient for the airmass term constant to achieve a reasonable transformation. As we are only interested in differential photometric results, this should not adversely affect the analysis of our data. Similarly, we did not calibrate our $H\alpha$ photometry to an absolute scale or calibrate for extinction as we were only interested in differential photometric results.

Due to the crowded nature of most of our clusters, unless otherwise noted, final cluster photometry was obtained using standard IRAF point-spread function (PSF) fitting techniques. The FWHM of typical point sources varied in a non-linear manner across the chip, thus we used a second order PSF function. Background sky levels were determined using mode statistics of an annulus of inner radius $4 * FWHM$ having a width of $3 * FWHM$. Since the PSF photometry routine used an aperture size, given by the average FWHM of stars in an image, which was much smaller than the 12 pixel radius used for the photometry of the standard fields, an aperture correction was applied.

Achieving excellent absolute photometric accuracy was not an inherent goal of this study; nonetheless, for each of our fields of view we compared our measured photometry of several bright sources to published values (cross-listed in SIMBAD or McSwain & Gies 2005b) to search for signs of egregious systematic errors. Our NGC 2186 photometry was the only data which exhibited any evidence of systematic errors; these data are consistently ~ 1 V-band magnitude fainter than the photometric values cross-listed in SIMBAD. These data were taken through clouds, thus the cause of the observed systematic error is likely related to the incomplete modeling of these effects via our observations of standard star fields. We do not believe that these errors in the absolute photometry of NGC 2186 significantly affected our interpretation of the cluster’s differential photometric behavior.

After completing the photometry measurements for all of our data, we organized our observations of each cluster into groups of short, medium, and deep B,V,R, $H\alpha$ exposures (see Table 1). Note that multiple listings of $H\alpha$ exposures in a single grouping indicate that two separate $H\alpha$ images were obtained to allow for co-addition of results and hence lower errors. Repetitive listings of individual targets in the short, medium, and deep exposures

were identified and the observation having the lowest B-band error was selected for use in this study. Finally, the photometric data were transformed into the standard system using the transformation coefficients listed in Table 2.

3. Results

Following the techniques employed by Grebel, Keller, and others in the literature, we used a simple 2 color diagram (2-CD) technique to identify the candidate Be star populations in our clusters. First, the B, V, R, and $H\alpha$ photometry of all stars in a cluster were plotted on a 2-CD, as illustrated in Figure 1. Normal blue main sequence stars and most blue supergiants clumped in one section of this diagram, e.g. at $(B - V) = 0.0$ and $(R - H\alpha) = -5.7$ in Figure 1, while red main sequence and red supergiant stars associated in another region, e.g. at $0.3 < (B - V) < 1.5$ and $(R - H\alpha) = -5.7$ in Figure 1. Blue stars which showed excess $H\alpha$ emission, e.g. $(R - H\alpha) > -5.54$ in Figure 1, were designated *candidate* Be stars. Three criteria were used to delineate candidate Be stars from other astrophysical objects: (B-V) colors, (R- $H\alpha$) colors, and m_V magnitudes.

Our choice of maximum (B-V) colors delineating candidate Be stars from other astrophysical objects was based on the possible range of colors of classical Be stars in our clusters. B-type stars of luminosity class III to V should exhibit unreddened (B-V) colors of $-0.3 < (B - V) < \sim 0$ (FitzGerald 1970; Landolt-Bornstein 1982). Classical Be disks can further redden the observed (B-V) colors by a few tenths of a magnitude (Schild 1978); furthermore, interstellar reddening, as measured by the mean $E(B-V)$ of our clusters (see Table 1), will also redden the aforementioned nominal color range. However, this mean $E(B-V)$ does not accurately characterize the reddening experienced by all cluster members. For example, while Olsen et al. (2001) cite a mean $E(B-V)$ of 0.09 for LH 72, individual targets were observed to have $E(B-V)$ values ranging from 0.04 to 0.22. Thus some cluster objects may experience an additional reddening of about the same order as the quoted cluster mean $E(B-V)$. The (B-V) color cutoffs we used to identify candidate Be stars were $(-0.3 + x + y + z) < (B - V) < (\sim 0 + x + y + z)$; where x represents the amount of reddening from Be disks (~ 0.2), y is the mean $E(B-V)$ for each cluster, and z incorporates the possible affects of additional patchy interstellar reddening (1 times the quoted mean $E(B-V)$). We stress that these cutoffs are only approximations meant to identify likely candidate Be stars; follow-up observations of these targets, especially the few which lie on the borders of our chosen cutoffs, will be needed to confirm their status as bona-fide classical Be stars. We will discuss individual (B-V) cutoffs for each of our clusters in the following subsections.

The choice of (R- $H\alpha$) colors delineating candidate Be stars from normal main sequence

stars is somewhat arbitrary, and there is no systematic cutoff used throughout the myriad of literature studies which use 2-CDs to investigate classical Be populations. McSwain & Gies (2005a) recently introduced an analysis technique based on synthetic photometry and empirical colors to alleviate such concerns, but this technique has yet to be widely adopted. When assigning minimum (R-H α) cutoffs to our clusters, we tried to ensure that our candidates showed noticeably more excess H α emission than likely main sequence stars which had slightly redder (B-V) colors than those expected for B-type stars. Given the typical $(R - H\alpha)_{error}$ of less than 0.10 and the sometimes considerable dispersion present in the blue and red main sequence clumps, we suggest that our chosen $(R - H\alpha)$ cutoffs dividing blue main sequence stars from candidate Be stars represent a conservative estimate of candidate Be star populations. As expected, and as noted by other authors (e.g., Fabregat & Torrejon 2000), such a division will tend to exclude the detection of candidate Be stars which exhibit low levels of Balmer emission.

As a final constraint, we also ensured that the apparent magnitudes of candidate Be stars in each of our clusters coincided with those expected for B-type stars of luminosity class III-V. Using the distances and reddening values for our clusters, we determined the upper (using B0III $M_V = -5.1$, Landolt-Bornstein 1982) and lower (using A0V $M_V = 0.65$, Landolt-Bornstein 1982) limits of expected apparent magnitudes for candidate Be stars in our clusters.

Results for individual clusters are discussed below and summarized in Table 3. Photometric data for each candidate Be star identified in this study, as well as astrometric coordinates accurate to < 0.3 arc-seconds, are compiled in Table 4. Note that the reliability of each candidate Be star detection in each cluster was double-checked via inspection of each candidate’s contour plot and radial profile in multiple filters using IRAF. A number of initial detections located within dense pockets of H II nebular emission were disregarded as we believed their detection was the result of spurious background noise. We also identified numerous objects which we classified as “possible detections” (see column 10 in Table 4). Due to either their location in dense H II regions or possible nearby stellar contamination, we suggest these objects be observed with secondary techniques, such as polarimetry or spectroscopy, to confirm or discount their possible status as classical Be stars. Note that data tabulated within parentheses in Table 3 include both “firm” detections and “possible” detections of candidate Be stars.

3.1. Candidate Be Stars in SMC Clusters

3.1.1. *Bruck 60*

Based on the finder chart in Kontizas (1980), we defined the cluster size of Bruck 60 to be a circle of diameter $3'.0$. Candidate Be stars were identified as stars on the 2-CD (see Figure 1) with $(B - V) < 0.35$, $(R - H\alpha) > -5.54$, and $m_V > 13.9$. We identified 26 candidate Be stars based upon this selection criteria, with 5 of these (Bruck 60:WBBBe 7, 21, 23, 25, and 26) being classified as “possible detections”. The location of these candidate Be stars on the cluster color magnitude diagram (CMD) is given in Figure 2. Note that the CMD and 2-CD for Bruck 60 are presented here for illustration. For subsequent clusters, the detailed CMDs and 2-CDs will be available in the online version of the Journal. From an inspection of Bruck 60’s CMD, as well as those for our other clusters, one can see that our candidate Be stars sometimes lie redward of the main sequence by $(B-V) \sim 0.1$. This likely indicates the presence of a small amount of intrinsic reddening from these objects’ circumstellar environments, as expected.

3.1.2. *Bruck 107*

Kontizas (1980) defined membership in this cluster by a circle of diameter $3'.5$. We identified 12 candidate Be stars from this cluster’s 2-CD, using the selection criteria of $(B - V) < 0.20$, $(R - H\alpha) > -5.43$, and $m_V > 13.9$. Kontizas (1980) also defined a ring with an inner radius of $1'.75$ and outer radius of $2'.88$ as representative of the background field star population. Applying the same 2-CD selection criteria as for the cluster population, we found 7 candidate Be stars in this suggested background field population, with 1 of these detections (Bruck 107:WBBBe 16) classified as a “possible detection”. Note that in Table 4, candidate Be stars labeled Bruck 107:WBBBe 13-19 correspond to these field stars.

3.1.3. *HW 43*

Kontizas (1980) defined cluster membership in HW 43 by a circle of diameter $3'.0$. Seven stars with $(B - V) < 0.20$, $(R - H\alpha) > -5.50$, and $m_V > 13.9$ in this cluster’s 2-CD were designated as candidate Be stars.

3.1.4. NGC 371

The cluster size for NGC 371 was taken from the work of Hodge (1985) and Massey, Waterhouse, & DeGioia-Eastwood (2000), $7'.0 \times 9'.0$. The original cluster definition in Hodge (1985) was a pseudo-potato shape whose major-minor axis alignment was almost N-E. We have used a $7'.0 \times 9'.0$ rectangle oriented N-E to approximate this definition. Because of completeness issues, we excluded all stars fainter than $V = 18.50$ from our analysis. 129 candidate Be stars were identified using the criteria $-0.40 < (B - V) < 0.50$ and $(R - H\alpha) > -5.45$. Note that NGC 371:WBBe 2 is 0.16 magnitudes too bright to be a B0III-B0V type star, given the distance modulus, R_V , and $E(B-V)$ of the cluster. However, follow-up polarimetric observations of this target (Wisniewski 2005; Wisniewski et al. 2006) clearly demonstrate that it is a classical Be star. We therefore included it in the present study and adopted a m_V magnitude cutoff of 13.8 for the cluster. 11 of these objects were designated as “possible detections”: NGC 371:WBBe 19, 54, 60, 64, 71, 87, 90, 96, 122, 127, 129.

3.1.5. NGC 456

The cluster size of $5'.0 \times 3'.2$ was based upon that used by Hill, Madore, & Freedman (1994a). 23 candidate Be stars were identified using the criteria $(B - V) < 0.5$, $(R - H\alpha) > -5.30$, and $m_V < 14.5$ and we consider 1 of these candidates as a “possible detection”, NGC 456:WBBe 21.

3.1.6. NGC 458

A circle of diameter $2'.17$ was used to define cluster membership (Matteucci et al. 2002) in NGC 458. We further excluded a small number of detections with $(B - V)_{error} > 0.175$. We assigned candidate Be star status to all objects with $-0.3 < (B - V) < 0.2$, $(R - H\alpha) > -5.42$, and $m_V < 13.9$ resulting in the identification of 30 objects. 2 “possible detections” were included in this total, NGC 458:WBBe 5 and 19.

3.1.7. NGC 460

The dimensions of this cluster, $4'.6 \times 6'.0$, were adopted from Hill, Madore, & Freedman (1994a). 21 candidate Be stars with $(B - V) < 0.2$, $(R - H\alpha) > -5.40$, and $m_V > 14.1$

were identified from this cluster’s 2-CD, with 7 identified as “possible detections”, NGC 460:WBBe 1, 9, 13, 14, 19, 20, and 21.

3.1.8. NGC 465

A cluster size of $5'.3 \times 5'.3$ was assumed based upon the definition of Hill, Madore, & Freedman (1994a). 11 candidate Be stars with $(B - V) < 0.25$, $(R - H\alpha) > -5.40$, and $m_V > 14.0$ were identified in this cluster’s 2-CD.

3.2. Candidate Be Stars in LMC Clusters

3.2.1. LH 72

The unique cluster shape designated by Lucke (1972), kindly supplied to us by K. Olsen (2003, private communication), was used to define LH 72 cluster membership. We eliminated all stars with $V > 18.7$ from our analysis owing to completeness issues. Candidate Be stars were defined as objects with $(B - V) < 0.4$, $(R - H\alpha) > -5.60$, and $m_V > 13.7$ in the cluster’s 2-CD, resulting in 50 detections. Note that 11 of the 50 candidate Be stars were designated “possible detections”: LH 72:WBBe 2, 15, 18, 20, 23, 37, 38, 41, 43, 46, and 48.

The Be population of this cluster and its nearby vicinity was previously investigated (Olsen et al. 2001), with a fractional Be population of “at least 10%” reported by these authors. We have attempted to correlate these previously suggested Be stars, using the x and y pixel coordinates kindly supplied to us by K. Olsen (2003, private communication), with the candidate Be stars identified in this study. With the exception of the two Be stars for which Olsen et al. (2001) listed RA and Dec coordinates, we were unable to make firm correlations between the data sets, and we suggest two explanations. As discussed in the introduction, Be stars are variable stars known to periodically enter quiescent phases in which they lose most or all of their circumstellar disks. Thus it is not unexpected that we might identify a different set of candidate Be stars than those identified from a previous epoch. LH 72 also resides in a region of significant $H\alpha$ nebulosity. It is likely that both Olsen et al. (2001) and the present study mis-identified a small number of candidate Be stars due to spurious detections induced by this diffuse, heterogeneous background. Each study also used a different method of accounting for this diffuse background emission; hence, one might expect that different types of mis-detections might be present in our study as compared to those present in Olsen et al. (2001).

3.2.2. NGC 1850

We defined the cluster dimensions of NGC 1850 to be $3'.8 \times 3'.8$. Vallenari et al. (1994) suggested that this region actually contains three distinct groupings of stars, NGC1850, NGC1850A, and H88-159, which are in slightly different evolutionary stages. Given the extremely crowded nature of the center of the field and the quality of our images, we were unable to accurately separate these cluster components and thus have considered the entire region as a single unit. Additionally, we have excluded all stars from our analysis which have $m_V > 18.50$, $m_V < 14.0$, $(R - H\alpha)_{error} > 0.10$, and $(B - V)_{error} > 0.18$.

Inspection of the cluster’s 2-CD reveals considerable noise, which we attribute to crowding effects. We therefore imposed very conservative candidate Be criteria of $-0.35 < (B - V) < 0.40$ and $(R - H\alpha) > -5.30$. Using these guidelines we identified 92 candidate Be stars, of which we classified 6 as “possible detections”: NGC 1850:WBBBe 4, 29, 52, 57, 58, and 84.

3.2.3. NGC 1858

The parallelogram cluster shape used by Vallenari et al. (1994) was used to define cluster membership in our observation of NGC 1858. We excluded all objects $V > 19.0$ from our analysis. 39 candidate Be stars were identified using the criteria that $-0.3 < (B - V) < 0.4$, $(R - H\alpha) > -0.30$, and $m_V > 13.9$ in this cluster’s 2-CD, with 4 candidates classified as “possible detections”: NGC 1858:WBBBe 9, 13, 24, and 35.

3.2.4. NGC 1955

The cluster size of $4'.2 \times 3'.5$ was based upon that used by Hill, Madore, & Freedman (1994a). Candidate Be stars were identified using the criteria $(B - V) < 0.25$, $(R - H\alpha) > -5.50$, and $m_V > 13.7$ leading to the detection of 24 targets. 3 of these targets were classified as “possible detections”: NGC 1955:WBBBe 9, 14, and 24.

3.2.5. NGC 2027

The cluster dimensions of $9'.0 \times 5'.0$ were adopted from Lucke & Hodge (1970). We excluded all stars with $V > 19.0$ from our analysis. Based on the selection criteria of $(B - V) < 0.3$, $(R - H\alpha) > -5.40$, and $m_V > 13.6$ we identified 46 candidate Be stars, of

which 3 were classified as “possible detections”: NGC 2027:WBBBe 44, 47, and 48.

3.2.6. *ELHC Fields 2,3*

Lamers, Beaulieu, & de Wit (1999) and de Wit, Beaulieu, & Lamers (2002) identified 21 EROS LMC Herbig Ae/Be (HAeBe) Candidates (ELHCs) by searching the EROS2 micro-lensing photometry database for irregular variables which exhibited similar properties to Galactic Herbig Ae/Be stars. We observed two LMC fields which contained many of these ELHCs to determine if they exhibited excess $H\alpha$ emission, as would be expected if they were truly intermediate-mass pre-main-sequence objects.

Since the ELHCs were dispersed across a significant portion of the LMC, we analyzed the stellar content of the full $13'.5 \times 13'.5$ field of view of both of the LMC fields we observed. We limited our analysis to stars with $m_V > 13.4$, $m_V < 19.0$, $(B - V)_{error} < 0.15$ and $(R - H\alpha)_{error} < 0.15$. For the ELHC field 2 image, we assigned the designation “candidate emission-line stars” to 183 stars having $(B - V) < 0.50$ and $(R - H\alpha) > -5.35$. We detected 4 of the 5 previously designated ELHCs in our field of view, ELHC 3, ELHC 4, ELHC 7, and ELHC 19; however, we note that 2 of these detections, ELHC 3 and ELHC 4, were very close to our minimum detection criteria. The star ELHC 20 (de Wit, Beaulieu, & Lamers 2002), which we observed to have $(R - H\alpha) = -5.61$, was not detected as a candidate emission-line star on our 2-CD. Figure 2.15, available in the online edition of this Journal, presents the CMD of this field of view; the four detected ELHC stars are plotted as large circles, while the remaining 179 “candidate emission-line stars” are not identified by any special type of symbol.

In our ELHC field 3 image, 153 “candidate emission-line stars” were identified using the criteria $(B - V) < 0.50$ and $(R - H\alpha) > -5.20$. We detected 5 of the 7 previously designated ELHCs in this field of view, ELHC 1, ELHC 6, ELHC 8, ELHC 12, and ELHC 13. ELHC 5, with $(R - H\alpha) = -5.39$, was not detected as a candidate on our 2-CD. We found ELHC 11 to be composed of two stellar components separated by $\sim 2''.4$. The $(R - H\alpha)$ magnitude of each of these components, -5.55 and -5.77 , lay outside of our selection criteria for candidate emission-line objects. Unfortunately we could not comment on the status of ELHC 9, which was also in this field of view, as it was centered on a significant cluster of bad columns on the CCD. Figure 2.16, available in the online edition of this Journal, presents the CMD of this field of view. The five detected ELHC stars are plotted as large circles in this figure, while the remaining 148 “candidate emission-line stars” are not identified by any special type of symbol.

3.3. Candidate Be Stars in Galactic Clusters

We also examined the fractional Be content of three Galactic clusters. Given the diffuse nature of these open clusters, we used aperture photometry to analyze these data.

3.3.1. NGC 2186

We observed this cluster, as in spite of its relatively young age, the WEBDA database (Mermilliod & Paunzen 2003) indicated that no one had identified its population of classical Be stars. We defined the cluster size as a $5'.8 \times 5'.2$ box which corresponds to the field considered by Moffat & Vogt (1975). Recall from Section 2 that our NGC 2186 data seem to suffer from systematic photometric errors which make all objects appear ~ 1 magnitude fainter than published photometry of the cluster. We have not corrected our data for these systematic effects; however, we do not believe these errors significantly affect our differential photometric results. Candidate Be star status was assigned to 5 stars with $(B - V) < 0.40$, $(R - H\alpha) > -4.80$, and $m_V < 14.0$. Note that in the absence of our systematic photometry errors, we would have applied a m_V cutoff of 13.0 for this cluster.

3.3.2. NGC 2383

At the time of our observations, no one had identified the Be population of NGC 2383 (Mermilliod & Paunzen 2003); subsequent to this time McSwain & Gies (2005b) have published a photometric study of the cluster in which they identified two Be stars, labeled as stars # 11 and # 341 in their survey. There is considerable disagreement in the literature concerning the age of NGC 2383 and the spectral classification of some of its members. Lynga (1987) claim the cluster's age is $\log(t) = 7.4$, while Subramaniam & Sagar (1999) claim a much older age of $\log(t) = 8.6$. The spectral classifications given in Subramaniam & Sagar (1999) also differ significantly from previous classification attempts, e.g. they classify their star S1 as an A3 I object versus a previous classification of B0 III.

Subramaniam & Sagar (1999) defined cluster membership to extend to a diameter of $5'.0$, which we also adopted. We identified 3 candidate Be stars on the cluster's 2-CD using the criteria $(B - V) < 0.40$ and $(R - H\alpha) > -5.78$. As there is a large uncertainty in the distance to this cluster, we did not define an upper m_V cutoff when determining this cluster's candidate Be star population. For similar reasons, we have not tabulated the number of B-type main sequence stars for this cluster in Table 3. Comparing our dataset to that of McSwain & Gies (2005b), one of their Be star detections (star # 341) was detected in the

present study as NGC 2383:WBBBe 1 while their other Be star detection (star # 11) was not detected by us. Our other two candidate Be star detections, NGC 2383:WBBBe 2 and 3, were not flagged as Be stars by McSwain & Gies (2005b).

3.3.3. NGC 2439

We adopted a cluster diameter of $10'.0$ based upon the cluster map of White (1975). We further restricted our analysis to stars with $(R - H\alpha)_{error} < 0.1$. Note that we strongly suspect that our group of shortest exposures of this cluster have uncertain exposure times due to the limited fastest shutter speed of the CTIO 0.9m. As a result, the few cluster stars we report from this set of exposures appear to be bluer by ~ 0.5 than the other exposure sets.

Slettebak (1985) and references therein note the presence of 5 Be stars in the cluster, labeled as stars 6, 69, 75, 81, and 303. We identified 4 of these 5 previously known Be stars, numbers 6, 69, 81, and 303, based on a 2-CD criteria of $(B - V) < 0.5$, $(R - H\alpha) > -5.80$, $m_V > 9.3$, and $m_V < 15.0$. Star number 41 (White 1975) also appeared as a candidate Be star in our data, although it was not previously detected as such. In contrast, the previously identified Be star number 75 in the study by Slettebak (1985) was not detected as such by our data set. More recently, McSwain & Gies (2005b) used 2-CDs to identify 6 Be and 7 candidate Be stars associated with NGC 2439. The present study has confirmed 4 of 6 of the Be detections reported by McSwain & Gies (2005b) (WBBBe 1 = their no. 58, WBBBe 2 = their no. 24, WBBBe 3 = their no. 101, WBBBe 4 = their no. 22) and 1 of the 7 candidate Be detections reported by McSwain & Gies (2005b) (WBBBe 5 = their no. 41). The variability in the number of detections and non-detections amongst these surveys is likely due in part to the variable nature of classical Be stars, and these comparisons provide support for the idea that the identification of candidate Be stars may be subject to such variability issues. Additional factors such as differences in the defined size of the cluster (i.e. McSwain & Gies 2005b versus the present study) also influence the reported fractional content of Be stars.

4. Discussion

In order to better probe the role of evolutionary age and/or metallicity may play in the development of the Be phenomenon, we approximated rough spectral types for our candidate Be stars on the basis of rough magnitude bins associated with spectral ranges. We first transformed the apparent magnitudes of our candidates to the absolute scale, using

the standard equation $m_V - M_V = 5 \log d - 5 + A_V$, where $A_V = R_V * E_{(B-V)}$. For LMC clusters we used a distance modulus of 18.5 (Westerlund 1990) and $R_V = 3.41$ (Gordon et al. 2003), while for SMC clusters we adopted a distance modulus of 18.9 (Westerlund 1990) and $R_V = 2.74$ (Gordon et al. 2003). For our Galactic clusters we assumed $R_V = 3.1$ and used a distance modulus of 11.31 for NGC 2186 (Moffat & Vogt 1975) and 13.24 for NGC 2439 (White 1975). $E_{(B-V)}$ values for most clusters are listed in Table 1. Due to the lack of available published reddening values for Bruck 60, Bruck 107, and HW 43, we assigned these clusters the mean reddening value for the SMC, 0.037, as determined by Schlegel, Finkbeiner, & Davis (1998). Following the work of Grebel (1997), we used the calibration for main sequence stars given in Table 5 of Zorec & Briot (1997) to transform the absolute magnitude of each of our candidate Be stars into a spectral type. As discussed by Grebel (1997), a large uncertainty is associated with such a transformation technique; hence, our estimated spectroscopic classifications should be considered only crude approximations.

We summarize these rough spectroscopic classifications for our LMC and SMC clusters in Table 5. In column 2 of Table 5, we assigned an age label to each cluster given by: 5 Myr < Age < 8 Myr = very young (vy), 10 Myr < Age < 25 Myr = young (y), and 32 Myr < Age < 158 Myr = old (o). Note that we classified LH 72 as “very young” (vy) although a range of ages have been suggested for this cluster (see Table 1). Given the suggested multiple epochs of star formation in NGC 1850 (see Section 3.3.2), we designated this cluster as “old?” (o?). We have included all photometrically identified candidate Be stars in Table 5, including those classified as “possible detections” in Table 3.

We have combined the results of Table 5 into two bins: “early-type” candidate Be stars, corresponding to rough spectral types B0-B3, and “later-type” candidate Be stars, corresponding to rough spectral types B4-B5. The results of this binning are given in Table 6, and we suggest that such averages should mask the general level of uncertainty associated with the spectral types we have assigned. Clusters with fewer than 20 B-type main sequence objects in either of these spectral bins were excluded from consideration to lessen the effects of small number statistics. The standard deviation errors quoted in Table 6 were calculated assuming the data followed a binomial distribution. We have also averaged the fractional Be content, binned to early- and later-type stars, of clusters having like age and metallicity properties, as summarized in Table 7. The uncertainties quoted in this table merely represent the propagation of the previously calculated standard deviations, i.e. $\sigma = N^{-0.5} (\sigma_i^2 + \sigma_{i+1}^2 + \dots)^{0.5}$.

4.1. Metallicity Effects

We first examined our dataset to identify any trends in the fractional candidate Be content as a function of metallicity. Following the work of Maeder, Grebel, & Mermilliod (1999), we first considered the fractional early-type (B0-B3) Be content of “young” clusters having ages of $7.0 < \log(t) < 7.4$. Data matching these criteria in Table 6 are plotted in Figure 3, where open circles correspond to literature data, filled circles correspond to data presented in this study, and crosses represent the average of all clusters’ fractional Be content within a metallicity bin. It is possible to find a wide range of reported metallicities for many of the individual clusters presented in this survey, as noted by Maeder, Grebel, & Mermilliod (1999); hence, following their example, we have chosen to represent all SMC clusters with one average metallicity and all LMC clusters with another average metallicity value. We also follow the practice of Maeder, Grebel, & Mermilliod (1999) of assigning single, average metallicity values to both Galactic clusters located exterior and interior to the Solar location (see Figure 3). We recognize that this is an oversimplification, but given the large scatter in the current available values for individual cluster metallicities, it seems the best approach at present.

From Figure 3, it is clear that there exists a wide range of $\text{Be} / (\text{B} + \text{Be})$ ratios within each metallicity bin. The systematic errors inherent in the use of the 2-CD technique undoubtedly contribute to this scatter; differences in the environmental properties of specific individual clusters also might influence the observed scatter of fractional Be content. However, it is clear that a trend in the fractional Be content with metallicity exists. This trend is better seen in Figure 4, where the filled circles represent the average fractional Be content of “young” clusters. The average fractional Be content of SMC metallicity clusters is $> 2\sigma$ higher than the average Galactic (interior or exterior) value, as documented in Table 7.

While Figure 4 shows the same general trend depicted by Maeder, Grebel, & Mermilliod (1999), we believe that the improved statistics provided by the present study significantly strengthens the claim of a trend with metallicity. The trend claimed by Maeder, Grebel, & Mermilliod (1999) was based upon the observation of one cluster in the SMC metallicity bin of $z=0.002$. The present study’s use of 4 SMC clusters reduces the average fractional Be content within this metallicity bin from 39% (Maeder, Grebel, & Mermilliod 1999) to 32%. We must note that our results are not inconsistent with the general conclusion reached by McSwain & Gies (2005b), who found no evidence of a metallicity trend in their study of Galactic clusters. As seen in Figure 4, we also observe little convincing evidence of a trend over the smaller metallicity range probed by Galactic clusters; however, evidence of a metallicity trend develops when one extends surveys to include broader regions of metallicity space, such as the LMC and SMC.

If one assumes that the fractional Be content of clusters depends on metallicity, then such a trend also should be apparent when examining clusters in age denominations other than “young” clusters. We have plotted the average fractional early-type Be content of “very young” clusters, depicted as open triangles, and “old” clusters, depicted as open squares, in Figure 4. Although the quality of available data for these age groups is severely limited, and no data exist for Galactic clusters, we suggest that the “very young” and “old” cluster data plotted in Figure 4 are not inconsistent with the Be phenomenon being more prevalent in low metallicity environments. We do recognize, however, that there is still some controversy over the metallicity effect. For example, the results of Martayan et al. (2006) find a Be fraction in the LMC cluster NGC 2004 which is about the same as the standard Galactic value of 17%. To resolve these lingering uncertainties, we strongly suggest that additional observations of clusters in these extreme age ranges must be made, spanning a wide range of metallicities, in order to provide the statistics necessary to more definitively identify any trend present.

4.2. Evolutionary Age Effects

Inspection of Tables 5, 6, and 7 clearly reveal that we have found a substantial number of candidate Be stars in clusters ranging in age from 5 Myr to 8 Myr. From Table 5, it is clear that these young clusters not only contain B0 type candidate Be stars, but they also have a significant number of later-type candidate Be objects. If the Be phenomenon develops in the second half of a B star’s main sequence lifetime, we would not expect to find B0 type stars, let alone B4-B5 type stars, in these very young clusters. Furthermore, the average fractional candidate Be content in these very young clusters, detailed in Table 7, is similar to the nominal frequency of the Be phenomenon in the Galaxy of 17% (Zorec & Briot 1997).

Clearly our present understanding of how the Be phenomenon is related to a star’s evolutionary age would be altered if we could establish that these very young *candidate* Be stars were not remnant pre-main-sequence star-disk systems. The similarities between the fractional candidate Be population found in these very young clusters with respect to the nominal frequency of the Be phenomenon observed in the Galaxy is interesting. Classical Be stars of such a young age clearly would not have spent enough time on the main sequence to significantly spin-up via the mechanism proposed by Meynet & Maeder (2000), or via mass transfer in a binary system (McSwain & Gies 2005b). Since it is widely accepted that the Be phenomenon is inherently tied to rapid rotation, our data seem to suggest that stars emerging from their pre-main-sequence phase must possess a wide range of rotational velocities; namely, a significant number of objects must be rotating near their critical breakup velocities at the zero-age-main-sequence (ZAMS). We will explore the true nature of many

of these extremely young candidate Be stars in a later paper.

From Table 7, it is clear that the fractional early-type Be content of “young” clusters is significantly higher than the nominal frequency of the Be phenomenon (17%); furthermore, the fractional later-type Be content of these clusters is significantly lower than the early-type content. Examining the fractional early- and later-type Be content of “old” clusters in Tables 6 and 7, we also find evidence that the Be phenomenon in these clusters is more prevalent than the nominal value of 17%. It is unclear from our dataset whether there is any difference between the frequency of early-type and later-type Be stars in these old clusters. Our detection of early-type objects in “old” clusters is very curious, and we can not find a simple explanation in the literature which explains why such objects would be detected. The slight enhancement of the fractional later-type Be content in our old clusters and the much larger enhancement of the fractional early-type Be content in our young clusters supports previous suggestions that the Be phenomenon is more prevalent in the later stages of a B star’s main sequence lifetime (Mermilliod 1982; Grebel 1997; Fabregat & Torrejon 2000; Keller 2004; McSwain & Gies 2005b). Recall however, that the results from our very young clusters indicate that such an evolutionary effect *may not* be the sole mechanism responsible for the development of the Be phenomenon.

We now consider the mechanisms which might be responsible for the observed evolutionary effect in the Be phenomenon. The detection of a sizable fraction of candidate Be stars in clusters younger than 10 Myr suggest that stars emerging onto the ZAMS might display a wide range of rotational rates, including stars which are rotating near their critical breakup velocity, hence exhibiting the Be phenomenon. The theoretical models of Meynet & Maeder (2000) and Maeder & Meynet (2001) illustrate that the ratio of angular velocity to critical angular velocity ($\Omega / \Omega_{critical}$) steadily increases throughout the main sequence lifetime of early-type B stars, which these authors suggest might explain why the Be phenomenon is more prevalent in the later part of a B star’s main sequence lifetime. While we agree that the general notion of an evolutionary spin-up provides a reasonable explanation for most of the observational properties documented here and in the literature, we also consider some of other implications of Meynet’s and Maeder’s models.

Table 8 lists the main sequence lifetimes predicted by the models of Meynet & Maeder (2000) and Maeder & Meynet (2001) for rotating and non-rotating stars. Interestingly, stars starting with an enhanced rotation rate on the ZAMS will experience a longer main sequence lifetime than stars of similar mass which start with a small or null rotation rate. Recall that the fundamental underlying mechanism believed to differentiate classical Be stars from “normal” B-type objects is rapid rotation. We speculate that the different main sequence lifetimes experienced by rapidly rotating versus slowly rotating B-type stars might

influence the observed enhancement of the Be phenomenon in the later stages of a star’s main sequence lifetime. Consider a SMC cluster of age 25 Myr, which Table 8 suggests will only have B3 or later-type “normal B stars” remaining on the main sequence, assuming they started on the ZAMS as slow rotators. In addition to B3 or later-type rapidly rotating classical Be stars, B2 type classical Be stars will also still reside on the main sequence when the cluster is 25 Myr old. Hence, the fractional Be content derived for this cluster via the 2-color diagram technique will not be comparing Be to normal B stars of a similar range of spectral types. The additional presence of B2 type Be stars in this cluster might inflate the observed fractional Be content.

Since clusters younger than 10 Myr old should still have their entire B0-B9 sequence present on the main sequence, regardless of whether one considers rapidly or non-rapidly rotating stars, we expect no enhancement of the Be phenomenon due to this effect. Conversely, we would expect that the expansion of main sequence lifetimes due to rotation will greatly affect clusters in the 16-26 Myr age range. In these clusters, “normal” B1-B2 stars which were slowly rotating when they reached the ZAMS would have evolved off of the main sequence. B1-B2 type classical Be stars, which were rotating much more rapidly when they reached the ZAMS, will still be observable on the main sequence, hence B1-B2 and B3-later type Be stars will be detected via 2-CDs. Because the Be phenomenon is most prevalent amongst B1-B2 type stars, one might expect a very large enhancement of the Be phenomenon to be detected in these clusters. When one considers the fractional Be content of older clusters, the Be phenomenon would likely still be enhanced by this effect, but to a lesser degree than clusters 16-26 Myr old, as the prevalence of the Be phenomenon is lower in later spectral types.

Our data are consistent with this speculative scenario. No strong enhancement in the Be phenomenon is seen in our very young clusters, while moderate and strong enhancements in the Be phenomenon are seen in our old and young clusters respectively. From Table 7, one might question why we observe early-type objects in our “old” clusters. We would expect that most slowly rotating early-type stars should have evolved off of the main sequence in these clusters. A limited number of early-type classical Be stars might still reside on the main sequence, owing to the extended main sequence lifetime afforded to rapid rotators. It is a little more difficult to explain the nature of early-type non-Be stars detected in these clusters; however, it is possible that these objects are blue stragglers. Note that the binary scenario for the formation of Be stars predicts that some should appear as blue stragglers (Pols et al. 1991); hence, if “normal” B-type blue stragglers populate these clusters, some of the clusters’ Be population may have their origin linked to binarity, not the suggested extension of main sequence lifetimes. It is clear that additional observations are needed to investigate the nature of both the early-type candidate Be stars and normal B stars in such

“old” clusters.

Differentiating between an enhancement in the Be phenomenon which is due to the spin-up of stars as they evolve along the main sequence versus an extension of the main sequence lifetime in rapidly rotating stars will likely be a difficult task. Of course, it is entirely possible that both mechanisms could play a role in producing the observed enhancements. One could examine the statistical distribution of rotational velocities of early-type versus later-type B stars in clusters spanning a range of ages to look for evidence of a systematic spin-up of the overall distribution with age. Conversely, if one could find numerous classical Be stars in a cluster having earlier spectral types than all of the normal main sequence stars present, this would provide evidence that the extended main sequence lifetimes of rapid rotators might contribute to the observed enhancements of the Be phenomenon. In practice, measuring the spectral types of classical Be stars to high accuracy is difficult, so this later type of observational undertaking would likely be challenging.

4.3. Galactic Clusters

We also used the calibration of Zorec & Briot (1997) to assign crude spectral types to the candidate Be stars we identified in our Galactic clusters (see Table 9). Due to the large uncertainty in the distance to NGC 2383, we have not attempted to convert the observed apparent magnitudes of this cluster’s candidate Be stars into spectral types. Recall that our NGC 2186 photometry includes systematic errors which make our targets appear ~ 1 magnitude too faint; to correct for these systematics, we have applied a 1 magnitude offset to our data to compute the spectral types listed in Table 9. As discussed in Section 3.3.3, we detected 4 of 5 previously identified Be stars in NGC 2439 via our 2-CD and 1 previously undetected candidate Be star. Spectral types for two of the known Be stars are given in Slettebak (1985): star White #6 (White 1975) is a B2 V, which generally agrees with our rough B0 classification of this object (NGC 2439:WBBe 1 in Table 4), and star White #81 (White 1975) is a B1 V, which generally agrees with our rough B0 classification of this star (NGC 2439:WBBe 2 in Table 4).

4.4. ELHC Fields

As previously described, we have detected ELHC # 1,3,4,6,7,8,12,13, and 19 as candidate emission-line objects via 2-CDs and failed to detect ELHC 5, 11, and 20. This 75% detection rate offers supporting evidence that ELHC stars might be bonafide pre-main-

sequence objects. Recent low-resolution spectroscopic and JHK photometric observations of some of these ELHCs (de Wit et al. 2005) have revealed that some objects might have nearby, previously unresolved neighbors; furthermore, the lack of a strong near IR excess and lack of forbidden emission lines has led these authors to question whether many of these ELHCs are truly Herbig Ae/Be stars or whether they are classical Be stars.

With respect to our results, we also had noted that ELHC 11 seemed to be comprised of 2 components. The low-resolution spectroscopy of ELHC 11 and 20, which were both not detected as emission-line objects in our study, revealed these sources to have $H\alpha$ absorption lines slightly filled in with emission (de Wit et al. 2005). Because the 2-CD technique fails to detect weak $H\alpha$ emitters, it is not surprising that we failed to detect these objects. Based on these results, we would predict that when spectroscopic observations of ELHC 5 are made, they will also reveal a partially filled in absorption line at $H\alpha$. In a future publication, we will present the results of moderate resolution spectroscopic and near-IR photometric observations of many of these ELHC stars which were obtained to further probe the true nature of these objects.

4.5. Limitations of the 2-CD technique

We briefly discussed some of the known limitations of the 2-CD technique in the Introduction, and now consider this situation in more detail. The 2-CD technique typically assumes that all stars within an appropriate range of colors that have a $(R-H\alpha)$ magnitude in excess of some threshold are “Be stars”. However, as many Galactic O, B, and A type supergiants are known to show frequent $H\alpha$ emission, one expects that the detection of such objects via the 2-CD technique would artificially inflate the number of detected “Be stars”. For example, Olsen et al. (2001) obtained follow-up spectroscopy of star S132 in the LMC cluster LH 72, which they identified as a Be star from a 2-CD, and classified this object as a B8 Ia star. The luminosity class of S132 excludes it, by definition, from being a classical Be star. Similarly, Keller et al. (1999) identified NGC 346:KWBBE 13 as a “Be star” via a 2-color diagram. Unfortunately this object is the well known HD 5980 Wolf-Rayet/Luminous Blue Variable system, thus it is abundantly clear that it has been mis-classified by the simple 2-CD method as a (classical) “Be star”. In principle, one would expect that the location of these objects on a CMD would identify them as “contaminants”; however, this is clearly not always the case. It is possible that these stars are background objects with respect to the clusters with which they have been associated. It is also possible that a significant amount of their radiation is attenuated by a localized region of dust. These two examples demonstrate that it is not unreasonable to expect OBA supergiants to “contaminate” 2-CD detections.

We suggest the frequency of contamination by such objects is likely to be greater when one uses the 2-CD technique to investigate field star populations (Keller et al. 1999, 2001), compared to cluster populations, as the evolutionary age of a cluster population should restrict the range of spectral types of OBA supergiants present.

Recent follow-up low-resolution spectroscopic and near IR photometric observations of some ELHCs (de Wit et al. 2005) have raised issues with their classification as Herbig Ae/Be objects. Even assuming the most pessimistic interpretation of the results of de Wit et al. (2005), i.e. that ELHC 7 is the only true Herbig Ae/Be star of these candidates as it is the only one which exhibits a large near IR excess, the implications of these results regarding the proper interpretation of 2-CDs can not be ignored. We detected ELHC 7 on a 2-CD as being an excess H α emitter; therefore, we have solid evidence that Herbig Ae/Be stars may be detected via this technique. Clearly, it is not sufficient to merely label all excess H α emitters detected via 2-CDs as “Be stars” as is nearly universally done in the literature. Given a cluster of sufficient age, and assuming coeval development, one would not expect to find any remaining pre-main-sequence stars; hence, this type of contamination may not be an issue. However, when examining the background field Be population surrounding a cluster using the 2-CD technique (see Keller et al. 1999), we assert that one must be wary of detecting Herbig Ae/Be stars, which would serve to artificially inflate the ratio of detected classical Be stars.

Keller et al. (2000), Olsen et al. (2001), Olsen (2003, private communication), and the present study all found evidence that diffuse background contamination likely inflates the number of true classical Be stars detected via the 2-CD technique. A typical form of these spurious detections we encountered were random, quasi point-source-like pockets of emission which were misconstrued as stars, especially when the *daofind* image roundness parameters were slightly relaxed. One also might consider how diffuse sky nebulosity affects the measurement of real sources. The IRAF photometry methods we used sampled the sky background within an annulus of a given radius around sources and used the median pixel value as an estimate of the background. In extremely variable backgrounds, for example containing H II filamentary structures, it is not always clear that this technique fully accounts for the true background present. While we do not propose a better technique to estimate background fluxes in regions of complex nebulosity, we feel it is important to remind the reader of some of the difficulties associated with observations of embedded objects when considering the results of these and similar 2-CD investigations. The addition of other independent techniques, such as IR photometry and broadband or spectropolarimetry, could provide much needed cross-checks on such identifications.

5. Summary

We have presented B, V, R, and $H\alpha$ photometry of 5 LMC, 8 LMC, and 3 Galactic clusters. Plotting these data on 2 color diagrams, we identified the fractional content of candidate Be stars in each cluster, i.e the ratio of $Be/(B+Be)$. From these data we found:

1) Candidate Be stars appear in significant numbers in all clusters studied. We provide basic photometric information and astrometric RA and Dec coordinates for these candidate Be stars to facilitate follow-up investigations.

2) Four clusters with ages less than 10 Myr were found to have significant numbers of candidate Be stars, with crude spectral types ranging from B0 to B5. The fractional Be content of these young clusters was similar to the nominal value found in our Galaxy, $\sim 17\%$. Clearly, these results could dramatically alter our current understanding of the role evolutionary age plays in the development of the Be phenomenon *if* we can show that these objects are truly classical Be stars.

3) The fractional content of early-type candidate Be stars appears to be significantly enhanced in clusters of age 10-25 Myr old. Clusters older than 25 Myr also appear to have enhanced levels of early- and later-type candidate Be stars. We suggest that the spin-up of stars as they evolve along the main sequence and/or the enhanced main sequence lifetime of rapidly rotating stars compared to slow rotators may explain this effect.

4) From inspection of all B0 to B3 type candidate Be stars in clusters with ages 10-25 Myr, we find evidence that the Be phenomenon is more prevalent in low metallicity environments. The additional statistics present in this study lowers the average fractional Be content of SMC clusters from 39% (Maeder, Grebel, & Mermilliod 1999) to 32%.

5) We examined the Be population in two clusters, LH 72 and NGC 2439, which had their Be population previously investigated, and found evidence of previously unreported candidate Be stars. The variable nature of Be stars likely accounts for some of these differences, although spurious detections may play a more dominant role in explaining the differences observed in LH 72.

6) 75% of previously suggested ELHCs were detected as candidate emission-line objects via our 2-color diagrams. These detections: a) offer evidence that these objects do emit excess $H\alpha$ emission and hence offer supporting evidence that they might be pre-main-sequence objects; and b) illustrate that the 2 color diagram technique will identify other types of emission-line objects, besides classical Be stars.

7) We suggest that all objects identified by our 2 color diagrams, as well as similarly identified objects in the literature, should be classified as “candidate Be stars”. Herbig

Ae/Be, B[e], and OBA supergiants, which are of a fundamentally different nature than classical Be stars, often exhibit H α emission and thus also may be detected via the 2-CD technique. Complementary techniques, such as polarimetry, IR photometry, and optical/IR spectroscopy can help to remove some of this potential confusion.

We thank the referee, Douglas Gies, for comments which helped to improve this paper. We also thank the NOAO TAC for awarding observing time for this project. JPW acknowledges support from a NASA GSRP fellowship (NGT5-50469) and thanks NOAO for supporting his travel to CTIO. KSB is a Cottrell Scholar of the Research Corporation and gratefully acknowledges their support. This work has been supported in part by NASA LTSA grant NAG5-8054 to the University of Toledo. This research has made use of the SIMBAD database operated at CDS, Strasbourg, France, and the NASA ADS system.

REFERENCES

- Alcaino, G., Alvarado, F., Borissova, J., & Kurtev, R. 2003, *A&A*, 400, 917
- Bianchi, L., Hutchings, J.B., Massey, P. 1996, *AJ*, 111, 2303
- Bjorkman, J.E. & Cassinelli, J.P. 1993, *ApJ*, 409, 429
- Bjorkman, K.S., Miroshnichenko, A.S., McDavid, D., & Pogrosheva, T.M. 2002, *ApJ*, 573, 812
- Cassinelli, J.P., Brown, J.C., Maheswaran, M., Miller, N.A., & Telfer, D.C. 2002, *ApJ*, 578, 951
- Cranmer, S.R. 2005, *ApJ*, 634, 585
- Dieball, A. & Grebel, E.K. 1998, *A&A*, 339, 773
- Dolphin, A.E. & Hunter, D.A. 1998, *AJ*, 116, 1275
- Fabregat, J. & Torrejon, J.M. 2000, *A&A*, 357, 451
- Feast, M.W. 1972, *MNRAS*, 159, 113
- FitzGerald, M. Pim 1970, *A&A*, 4, 234
- Fullerton, A.W. et al. *ApJL*, 538, 43
- Garmany, C.D. & Conti, P.S. 1985, *ApJ*, 293, 407

- Gilmozzi, R., Kinney, E.K., Ewald, S.P., Panagia, N., & Romaniello, M. 1994, *ApJL*, 435, L43
- Gordon, K.D., Clayton, G.C., Misselt, K.A., Landolt, A.U., & Wolff, M.J. 2003, *ApJ*, 594, 279
- Grebel, E.K., Richtler, T., & de Boer, K.S. 1992, *A&A*, 254, L5
- Grebel, E.K. 1997, *A&A*, 317, 448
- Grebel, E.K. & Chu, Y. 2000, *AJ*, 119, 787
- Hill, R.J., Madore, B.F., & Freedman, W.L. 1994a, *ApJS*, 91, 583
- Hill, R.J., Madore, B.F., & Freedman, W.L. 1994b, *ApJ*, 429, 192
- Hillenbrand, L.A., Massey, P., Strom, S.E., & Merrill, K.M. 1993, *AJ*, 106, 1906
- Hodge, P. 1983, *ApJ*, 264, 470
- Hodge, P. 1985, *PASP*, 97, 530
- Hoffleit, D. & Jaschek, C. 1982, *The Bright Star Catalog*, Yale University Observatory
- Hoffleit, D., Saladyga, M., & Wlasuk, P. 1983, *A Supplement to the Bright Star Catalog*, Yale University Observatory
- Hummel, W. et al. 1999, *A&AL*, 352, L31
- Jaschek, M., Slettebak, A., & Jaschek, C. 1981, *Be Star Newsletter*, 4, 9
- Keller, S.C. & Bessell, M.S. 1998, *A&A*, 340, 397
- Keller, S.C., Wood, P.R., & Bessell, M.S. 1999, *A&AS*, 134, 489
- Keller, S.C., Bessell, M.S., & Da Costa, G.S. 2000, *AJ*, 119, 1748
- Keller, S.C., Grebel, E.K., Miller, G.J., & Yoss, K.M. 2001, *AJ*, 122, 248
- Keller, S.C. 2004, *PASA*, 21, 310
- Kontizas, M. 1980, *A&AS*, 40, 151
- Kudritzki, R.P., Cabanne, M.L., Husfeld, D., Niemela, V.S., Groth, H.G., Puls, J., & Her-rero, A. 1989, *A&A*, 226, 235

- Lamers, H.J.G.L.M., Beaulieu, J.P., & de Wit, W.J. 1999, *A&A*, 341, 827
- Landolt-Bornstein 1982, *Astronomy & Astrophysics Vol 2.*, ed. K. Schaifers & H.H. Voigt (Springer, Berlin)
- Landolt, A.U. 1992, *AJ*, 104, 340
- Lucke, P.B. & Hodge, P.W. 1970, *AJ*, 75, 171
- Lucke, P.B. 1972, Ph.D. thesis, University of Washington
- Lynga, G. 1987, *Catalog of Open Star Cluster Data* (Strasbourg: CDS)
- Maeder, A. 1999, *A&A*, 347, 185
- Maeder, A., Grebel, E.K., & Mermilliod, J-C. 1999, *A&A*, 346, 459
- Maeder, A. & Meynet, G. 2001, *A&A*, 373, 555
- Martayan, C., Fremat, Y., Hubert, A.-M., Floquet, M., Zorec, J., & Neiner, C. 2006, *A&A*, 452, 273
- Massey, P., Parker, J.W., & Garmany, C.D. 1989, *AJ*, 98, 1305
- Massey, P., Waterhouse, E., & DeGioia-Eastwook, K. 2000, *AJ*, 119, 2214
- Matteucci, A., Ripepi, V., Brocato, E., & Castellani, V. 2002, *A&A*, 387, 861
- Mazzali, P.A., Lennon, D.J., Pasian, F., Marconi, G., Baade, D., & Castellani, V. 1996, *A&A*, 316, 173
- McSwain, M.V. & Gies, D.R. 2005a, *ApJ*, 622, 1052
- McSwain, M.V. & Gies, D.R. 2005b, *ApJS*, 161, 118
- Mermilliod, J.-C. 1982, *A&A*, 109, 48
- Mermilliod, J.-C. & Paunzen, E. 2003, *A&A*, 410, 511
- Meynet, G. & Maeder, A. 2000, *A&A*, 361, 101
- Moffat, A.F.J. & Vogt, N. 1975, *A&AS*, 20, 85
- Olsen, K.A.G., Kim, S., & Buss, J.F. 2001, *AJ*, 121, 3075
- Owocki, S.P., Cranmer, S.R., & Gayley, K.G. 1996, *ApJL*, 472, 1150

- Penny, L.R., Sprague, A.J., Seago, G., & Gies, D.R. 2004, *ApJ*, 617, 1316
- Pols, O.R., Cote, J., Waters, L.B.F.M., & Heise, J. 1991, *A&A*, 241, 419
- Porter, J.M. 1996, *MNRAS*, 280, 31
- Porter, J.M. & Rivinius, T. 2003, *PASP*, 115, 1153
- Quirrenbach, A. et al. 1997, *ApJ*, 479, 477
- Rivinius, Th., Baade, D., Stefl, S., Townsend, R.H.D., Stahl, O., Wolf, B. & Kaufer, A. 2001, *A&A*, 369, 1058
- Schild, R.E. 1978, *ApJS*, 37, 77
- Schlegel, D.J., Finkbeiner, D.P., & Davis, M. 1998, *ApJ*, 500, 525
- Slettebak, A. 1985, *ApJS*, 59, 769
- Struve, O. 1931, *ApJ*, 73, 94
- Subramaniam, A. & Sagar, K. 1999, *AJ*, 117, 937
- Telting, J.H. 2000, in *The Be Phenomenon in Early-Type Stars*, ed. M.Smith, H. Henrichs, & J. Fabregat, *ASP Conf. Proc.*, 214, 422
- Townsend, R.H.D., Owocki, S.P., & Howarth, I.D. 2004, *MNRAS*, 350, 189
- Vallenari, A., Aparicio, A., Fagotto, F., Chiosi, C., Ortolani, S., & Meylan, G. 1994, *A&A*, 284, 447
- Westerlund, B.E. 1990, *A&A Rev.*, 2, 29
- White, S.D.M. 1975, *ApJ*, 197, 67
- Wisniewski, J.P. 2005, PhD Thesis, University of Toledo
- Wisniewski, J.P., Bjorkman, K.S., & Magalhães, A.M. 2006, in prep
- de Wit, W.J., Beaulieu, J.P. , & Lamers, H.J.G.L.M. 2002, *A&A*, 395, 829
- de Wit, W.J., Beaulieu, J.P., Lamers, H.J.G.L.M., Coutures, C., & Meeus, G. 2005, *A&A*, 432, 619
- Wood, K., Bjorkman, K.S., & Bjorkman, J.E. 1997, *ApJ*, 477, 926

Zorec, J. & Briot, D. 1997, A&A, 318, 443

Fig. Set 1. 2 Color Diagrams (2-CDs)

Fig. Set 2. Color Magnitude Diagrams

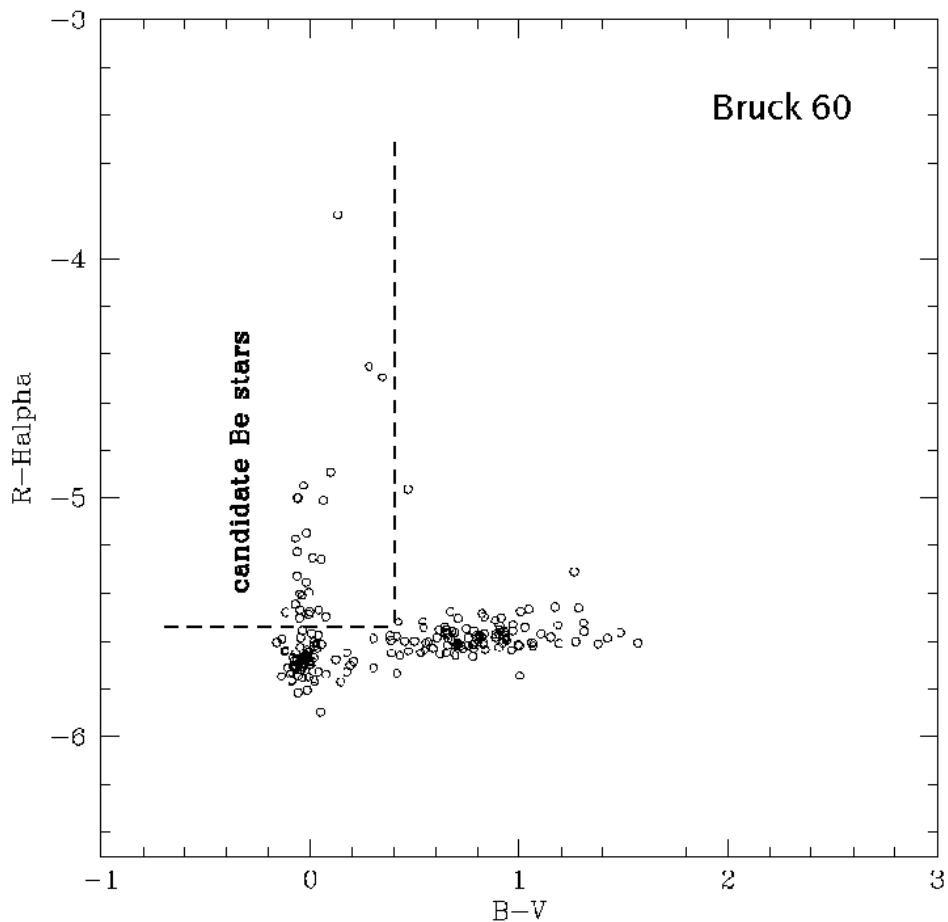


Fig. 1.— Following the techniques established by e.g. Grebel and Keller, we use 2 color diagrams to identify candidate Be stars in our observed clusters. Here we show an example 2-CD for the cluster Bruck 60. The online version of this paper includes additional 2-CD figures for the clusters: (F1.2) Bruck 107, (F1.3) Bruck 107 background population, (F1.4) HW 43, (F1.5) NGC 371, (F1.6) NGC 456, (F1.7) NGC 458, (F1.8) NGC 460, (F1.9) NGC 465, (F1.10) LH 72, (F1.11) NGC 1850, (F1.12) NGC 1858, (F1.13) NGC 1955, (F1.14) NGC 2027, (F1.15) ELHC Field 2, (F1.16) ELHC Field 3, (F1.17) NGC 2186, (F1.18) NGC 2383, (F1.19) NGC2439.

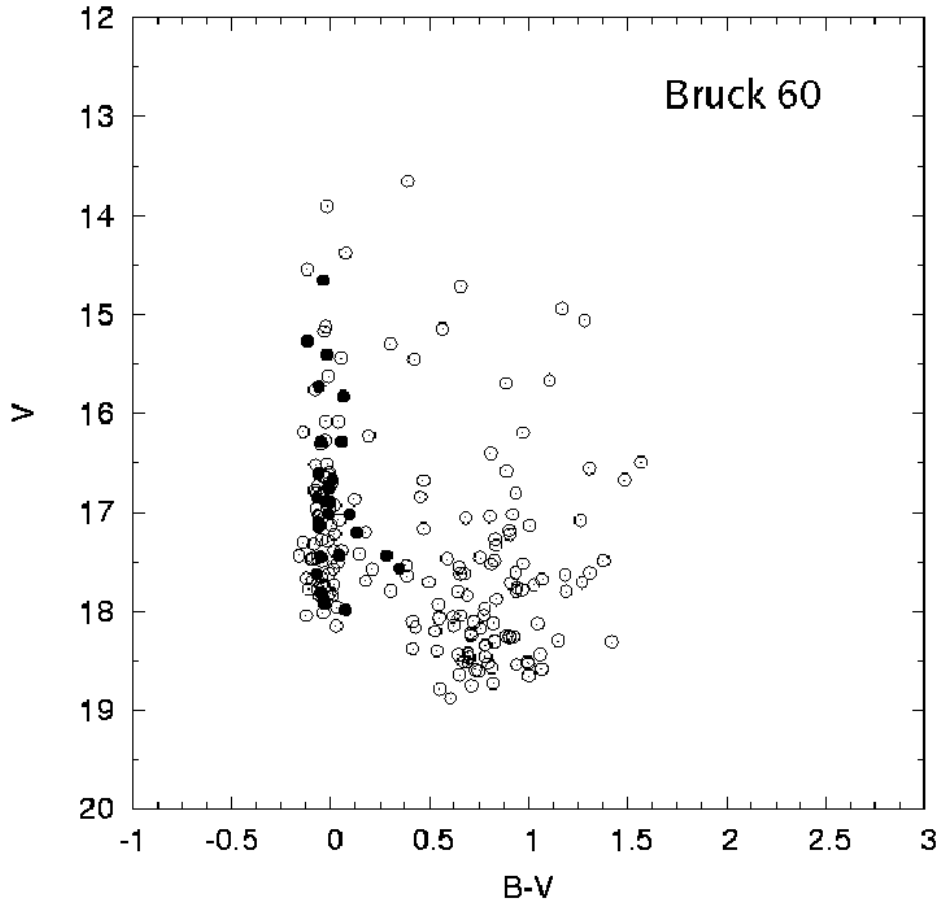


Fig. 2.— The CMD of the SMC cluster Bruck 60 is presented here. Filled circles represent the location of candidate Be stars identified in this study. Note that, as expected for classical Be stars, many candidates lie slightly to the right of the main-sequence. The online version of this paper includes CMDs for the clusters: (F2.2) Bruck 107, (F2.3) Bruck 107 background population, (F2.4) HW 43, (F2.5) NGC 371, (F2.6) NGC 456, (F2.7) NGC 458, (F2.8) NGC 460, (F2.9) NGC 465, (F2.10) LH 72, (F2.11) NGC 1850, (F2.12) NGC 1858, (F2.13) NGC 1955, (F2.14) NGC 2027, (F2.15) ELHC Field 2, (F2.16) ELHC Field 3, (F2.17) NGC 2186, (F2.18) NGC 2383, (F2.19) NGC 2439.

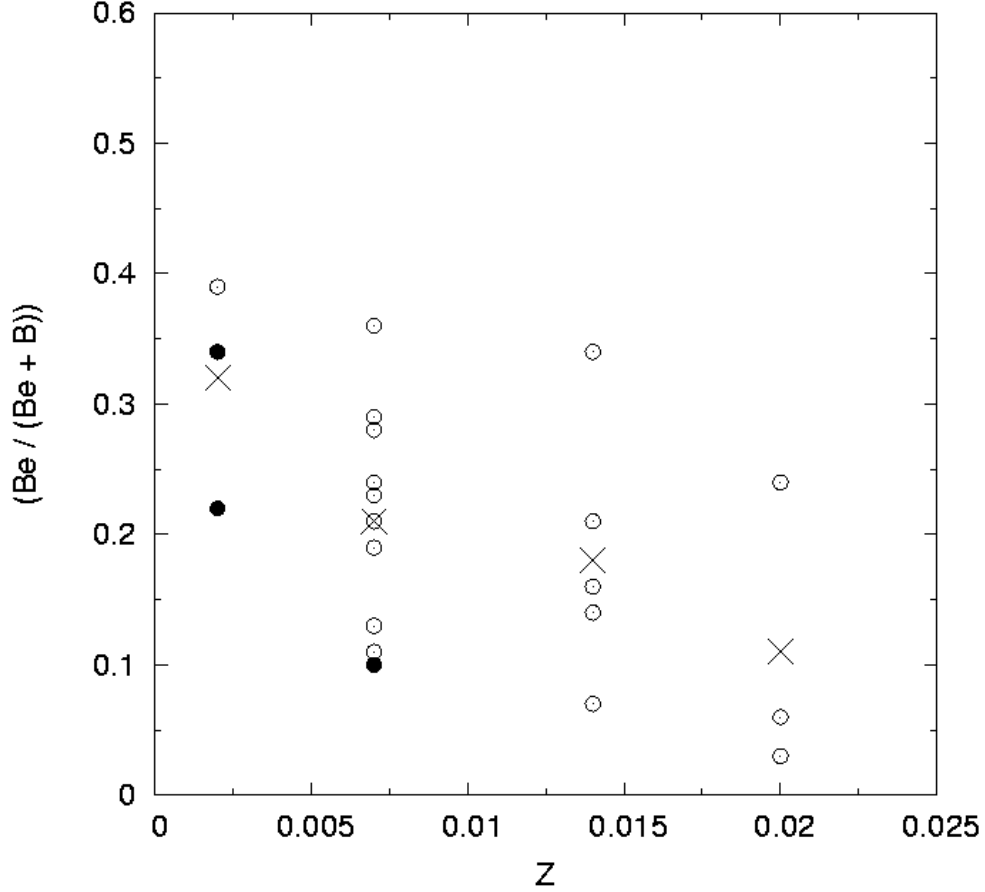


Fig. 3.— The fractional candidate Be star content of B0 - B3 type objects in “young” clusters with ages ranging from $7.0 < \log(t) < 7.4$ is shown as a function of cluster metallicity. Data from the present study, Keller et al. (1999), and Maeder, Grebel, & Mermilliod (1999) are plotted, excluding clusters which had fewer than 20 early-type (B + Be) stars. As discussed in Section 4.1, we have followed the practice of Maeder, Grebel, & Mermilliod (1999) and assigned average metallicity values for our SMC clusters ($z = 0.002$), LMC clusters ($z = 0.007$), Galactic clusters located exterior to the Solar location ($z = 0.014$), and Galactic clusters located interior to the Solar location ($z = 0.020$). The filled circles represent data presented in this study, the open circles represent literature data, and the large crosses represent the average of all cluster data within a metallicity bin.

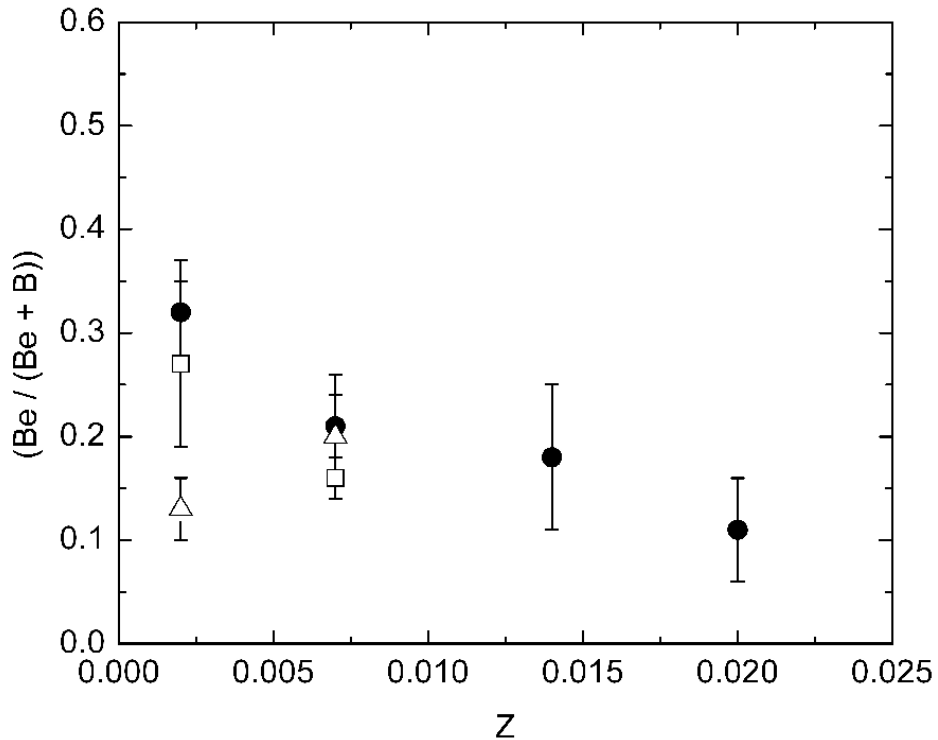


Fig. 4.— The fractional candidate Be content of clusters of various age denominations were averaged to examine systematic trends with metallicity. Open triangles correspond to “very young” clusters, closed circles correspond to “young” clusters, and open squares correspond to “old” clusters. As discussed in Section 4.1, we have followed the practice of Maeder, Grebel, & Mermilliod (1999) and assigned average metallicity values for our SMC clusters ($z = 0.002$), LMC clusters ($z = 0.007$), Galactic clusters exterior to the Solar location ($z = 0.014$), and Galactic clusters interior to the Solar location ($z = 0.020$).

Table 1: Basic Properties of the Observations

Cluster Name	Location	Date	Filter	Exposure Times	log Cluster Age	E(B-V)
ELHC-2 ³	LMC	2002 October 16	B,V,R,H α	60,15,15,120
...	B,V,R,H α ,H α	300,100,100,600,600
...	B,V,R,H α ,H α	300,300,300,600,600
ELHC-3 ⁴	LMC	2002 October 16	B,V,R,H α	60,15,15,120
...	B,V,R,H α ,H α	300,100,100,600,600
LH 72	LMC	2002 October 12	B,V,R,H α	60,15,15,120	6.7-7.2 ⁵	0.09 ⁵
...	B,V,R,H α ,H α	300,100,100,600,600
...	B,V,R,H α ,H α	600,600,600,600
NGC 1850	LMC	2002 October 13	B,V,R,H α	60,10,10,15	7.7 ^{1,7} -7.8 ^{1,6} , 6.6 ^{2,7} -6.9 ^{2,6}	0.18 ⁶
...	B,V,R,H α	300,100,100,120
...	B,V,R,H α ,H α	600,600,600,600,600
NGC 1858	LMC	2002 October 16	B,V,R,H α	60,15,15,120	6.9 ⁶	0.15 ⁶
...	B,V,R,H α ,H α	300,100,100,600,600
...	B,V,R,H α ,H α	600,100,600,600,600
NGC 1955	LMC	2002 October 14	B,V,R,H α	60,15,15,120	6.82 ⁸	0.09 ⁸
...	B,V,R,H α ,H α	600,300,300,600,600
NGC 2027	LMC	2002 October 15	B,V,R,H α	60,15,15,15	7.06 ⁸	0.05 ⁸
...	B,V,R,H α	300,100,100,120
...	B,V,R,H α ,H α	600,600,600,600,600
NGC 2186	MWG	2002 October 14	B,V,R,H α	30,15,15,20	7.738 ¹³	0.31 ¹⁵
...	B,V,R,H α	200,100,100,120
NGC 2383	MWG	2002 October 12	B,V,R,H α	5,5,5,10	7.4 ¹³ , 8.6 ¹⁴	0.22 ¹⁴
...	B,V,R,H α	30,30,30,60
...	B,V,R,H α	120,120,120,240
NGC 2439	MWG	2002 October 12	B,V,R,H α	3,5,3,3	7.3 ¹² , 7.82 ¹³	0.37 ¹²
...	B,V,R,H α	20,20,20,20
...	B,V,R,H α	120,120,120,120
Bruck 60	SMC	2002 October 15	B,V,R,H α	60,15,15,120	7.8 ¹¹	0.037 ¹⁸
...	B,V,R,H α ,H α	300,100,100,600,600
...	B,V,R,H α ,H α	600,600,600,600,600
Bruck 107	SMC	2002 October 15	B,V,R,H α	60,15,15,120	8.1 ¹¹	0.037 ¹⁸
...	B,V,R,H α ,H α	300,600,100,600,600
...	B,V,R,H α ,H α	600,600,600,600,600
HW 43	SMC	2002 October 13	B,V,R,H α	60,15,15,120	7.9 ¹¹	0.037 ¹⁸
...	B,V,R,H α ,H α	300,100,100,600,600
...	B,V,R,H α ,H α	600,600,600,600,600
NGC 371	SMC	2002 October 12	B,V,R,H α	60,15,15,120	6.74 ⁹	0.08 ⁹
...	B,V,R,H α ,H α	300,100,100,600,600
...	B,V,R,H α ,H α	600,600,600,600,600
NGC 456	SMC	2002 October 14	B,V,R,H α	60,15,15,120	7.0 ¹¹	0.27 ¹⁶
...	B,V,R,H α ,H α	300,100,100,600,600
...	B,V,R,H α ,H α	600,600,600,600,600
NGC 458	SMC	2002 October 13	B,V,R,H α ,H α	60,15,15,600,600	7.7 ¹¹ , 8.0-8.18 ¹⁰	0.04 ¹⁷
...	B,V,R,H α ,H α	300,100,100,600,600
...	B,V,R,H α ,H α	600,600,600,600,600
NGC 460	SMC	2002 October 16	B,V,R,H α	60,15,15,120	7.3 ¹¹	0.12 ¹⁶
...	B,V,R,H α ,H α	300,100,100,600,600
...	B,V,R,H α ,H α	600,600,600,600,600
NGC 465	SMC	2002 October 16	B,V,R,H α	60,15,15,120	...	0.09 ¹⁶
...	B,V,R,H α ,H α	300,100,100,600,600
...	B,V,R,H α ,H α	600,600,600,600,600

Note. — Summary of our CTIO 0.9 m photometric observations. Note that ¹ refers to NGC 1850A and ² refers to NGC 1850B. ³ and ⁴ denote observations of LMC fields which were reported to contain candidate HAeBe stars (Lamers, Beaulieu, & de Wit 1999; de Wit, Beaulieu, & Lamers 2002). ¹⁸ denote clusters for which no E(B-V) value was found in the literature, thus we assign the mean reddening value for the SMC determined by Schlegel, Finkbeiner, & Davis (1998) to these clusters. References cited are: ⁵ Olsen et al. (2001), ⁶ Vallenari et al. (1994), ⁷ Gilmozzi et al. (1994), ⁸ Dolphin & Hunter (1998), ⁹ Massey, Waterhouse, & DeGioia-Eastwood (2000), ¹⁰ Matteucci et al. (2002), ¹¹ Hodge (1983), ¹² White (1975), ¹³ Lynga (1987), ¹⁴ Subramaniam & Sagar (1999), ¹⁵ Moffat & Vogt (1975), ¹⁶ Hill, Madore, & Freedman (1994b), ¹⁷ Alcaino et al. (2003)

Table 2: Coefficients of Standard Star Transformations

Date	B ₀	B ₁	B ₂
2002 October 12	2.537 ±0.016	0.30	0.118 ±0.019
2002 October 13	2.246 ±0.015	0.30	0.109 ±0.019
2002 October 14	2.258 ±0.014	0.30	0.132 ±0.017
2002 October 15	2.477 ±0.041	0.30	0.076 ±0.052
2002 October 16	2.231 ±0.007	0.30	0.093 ±0.009
...	V ₀	V ₁	V ₂
2002 October 12	2.467 ±0.012	0.15	-0.010 ±0.014
2002 October 13	2.101 ±0.012	0.15	-0.017 ±0.015
2002 October 14	2.119 ±0.008	0.15	-0.023 ±0.010
2002 October 15	2.324 ±0.030	0.15	-0.295 ±0.049
2002 October 16	2.086 ±0.006	0.15	-0.018 ±0.007
...	R ₀	R ₁	R ₂
2002 October 12	2.495 ±0.019	0.08	0.077 ±0.040
2002 October 13	2.206 ±0.011	0.08	-0.001 ±0.021
2002 October 14	2.216 ±0.006	0.08	-0.016 ±0.013
2002 October 15	2.224 ±0.020	0.08	-0.013 ±0.043
2002 October 16	2.206 ±0.005	0.08	-0.015 ±0.011

Note. — Photometric transformation coefficients.

Table 3: Summary of Detected Candidate Be Stars

Cluster	V<14	V14	V15	V16	V17	V18	V≥19	# Be	# MS
Bruck 60	0/1	1/3	4/9	7(8)/29	9(13)/53	0/3	0/0	21(26)	98
Bruck 107 ¹	0/0	1/1	1/1	1/5	5/11	4/21	0/2	12	41
Bruck 107 ²	0/0	1/2	0/1	2/5	0/6	3(4)/19	0/2	6(7)	35
HW 43	0/0	0/0	0/0	0/1	1/11	4/31	2/9	7	52
LH 72	0/4	5(6)/22	7/40	5(9)/63	15(17)/86	7(11)/71	0/0	39(50)	286
NGC 371	1/4	9/52	11(12)/124	33(35)/250	43(47)/432	21(25)/222	0/0	118(129)	1084
NGC 456	0/0	3/4	1/5	3/16	12(13)/32	1/28	2/5	22(23)	90
NGC 458	0/0	0/0	0/4	2/4	4(6)/25	19/58	3/7	28(30)	98
NGC 460	0/0	1(2)/7	3(5)/16	2(3)/19	6(8)/36	2(3)/17	0/0	14(21)	95
NGC 465	0/0	1/14	3/22	1/32	4/75	1/65	1/7	11	215
NGC 1850	0/0	1/45	5/41	19(20)/134	44(49)/199	17/72	0/0	86(92)	492
NGC 1858	0/1	1/13	5/21	12(15)/37	16(17)/35	1/2	0/0	35(39)	109
NGC 1955	0/3	0/10	1/23	5/44	13(15)/46	2(3)/15	0/0	21(24)	141
NGC 2027	3/10	4/51	10/78	11/143	11/245	4(7)/324	0/0	43(46)	851
ELHC 2 ³	0/11 ⁵	3/37 ⁵	13/77 ⁵	36/341 ⁵	78/1013 ⁵	53/771 ⁵	0/0 ⁵	183 ⁵	2250 ⁵
ELHC 3 ⁴	1/14 ⁵	7/67 ⁵	24/151 ⁵	35/613 ⁵	55/1654 ⁵	31/1137 ⁵	0/0 ⁵	153 ⁵	3636 ⁵
NGC 2186	5/9	0/0	0/0	0/0	0/0	0/0	0/0	5	9
NGC 2383	3/14	0/26	0/48	0/18	0/0	0/0	0/0	3	... ⁶
NGC 2439	4/73	1/58	0/0	0/0	0/0	0/0	0/0	5	131

Note. — A summary of candidate Be stars found in this study, grouped in bins of observed V magnitude. Data in the V15 column, for example, correspond to candidate Be stars having $15.0 \leq V \leq 15.9$. Detection summaries listed in parenthesis are “possible detections” and should be viewed as less reliable than detection summaries without parenthesis. ¹ assumes a cluster diameter of 3.5 arc-minutes. ² is based upon a ring located at a radius of 1'.75 to 2'.88 from the cluster center, which Kontizas (1980) claim represents the background population. ³ and ⁴ represent observations of LMC fields which Lamers, Beaulieu, & de Wit (1999) and de Wit, Beaulieu, & Lamers (2002) claim contain numerous candidate Herbig Ae/Be stars. ⁵ indicates the detection of “candidate emission-line stars” and is not meant to reflect the field’s classical Be star content. ⁶ The number of B-type main sequence stars in NGC 2383 is not calculated, owing to the large uncertainty in the distance to this cluster.

Table 4: Photometric Properties of the Candidate Be Stars

Name	RA (2000)	Dec (2000)	V	V_{err}	(B-V)	$(B-V)_{err}$	(R-H α)	$(R-H\alpha)_{err}$	Status
Bruck 60:WBBBe 1	0 51 44.0	-73 14 27.7	16.88	0.02	-0.02	0.02	-5.35	0.04	C
Bruck 60:WBBBe 2	0 51 58.8	-73 15 3.1	16.67	0.01	0.01	0.01	-5.25	0.03	C
Bruck 60:WBBBe 3	0 51 35.4	-73 12 42.1	16.29	0.01	-0.05	0.01	-5.47	0.02	C
Bruck 60:WBBBe 4	0 51 31.8	-73 13 9.2	17.02	0.02	-0.01	0.02	-5.49	0.05	C
Bruck 60:WBBBe 5	0 51 42.8	-73 13 27.4	15.83	0.01	0.07	0.01	-5.01	0.02	C

Note. — A full version of this table will appear in the online Journal. The “Status” column designates the Be star classification we have assigned each object, “C” = candidate Be stars and “P” = possible candidate Be star.

Table 5: Spectral Types of Candidate Be Stars in Every Cluster Environment

Cluster	Age	B0	B1	B2	B3	B4	B5
NGC 371	vy	19/158 (12%)	16/136 (12%)	35/265 (13%)	16/177 (9%)	29/202 (14%)	14/146 (10%)
LH 72	vy	11/48 (23%)	3/32 (9%)	9/50 (18%)	5/28 (18%)	8/41 (20%)	7/34 (21%)
NGC 1858	vy	5/34 (15%)	6/18 (33%)	14/30 (47%)	8/13 (62%)	5/12 (42%)	1/2 (50%)
NGC 1955	vy	0/23 (0%)	2/24 (8%)	4/33 (12%)	3/16 (19%)	9/23 (39%)	4/18 (22%)
NGC 456	y	6/14 (43%)	2/13 (15%)	7/19 (37%)	5/12 (42%)	1/18 (6%)	0/10 (0%)
NGC 460	y	7/23 (30%)	2/11 (18%)	4/26 (15%)	3/13 (23%)	5/17 (29%)	0/3 (0%)
NGC 2027	y	13/92 (14%)	4/57 (7%)	9/110 (8%)	6/70 (9%)	5/116 (4%)	2/103 (2%)
Bruck 60	o	4/11 (36%)	3/10 (30%)	10/30 (30%)	5/22 (23%)	4/24 (17%)	0/1 (0%)
Bruck 107	o	2/2 (100%)	1/4 (25%)	0/3 (0%)	2/3 (67%)	3/6 (50%)	0/5 (0%)
HW 43	o	0/0 (0%)	0/0 (0%)	0/3 (0%)	1/2 (50%)	1/9 (11%)	2/6 (30%)
NGC 458	o	0/1 (0%)	0/3 (0%)	2/6 (30%)	3/11 (27%)	3/15 (20%)	7/24 (29%)
NGC 1850	o?	4/82 (5%)	7/57 (12%)	28/139 (20%)	17/72 (24%)	25/100 (25%)	11/42 (26%)
NGC 465	...	4/33 (12%)	1/22 (5%)	1/34 (3%)	1/27 (4%)	3/43 (7%)	0/21 (0%)

Note. — Spectral types were assigned using the calibrations of Zorec & Briot (1997), following the methods outlined by Grebel (1997): $B_0 : M_V < -3.25$, $B_1 : -3.25 < M_V < -2.55$, $B_2 : -2.55 < M_V < -1.8$, $B_3 : -1.8 < M_V < -1.4$, $B_4 : -1.4 < M_V < -0.95$, $B_5 : -0.95 < M_V < -0.6$. Grebel (1997) offers an excellent discussion of the numerous uncertainties inherent in assigning spectral types via this technique. In column 2, we group clusters into 3 age groups: very young (vy) : $6.7 < \log(t) < 6.9$; young (y): $7.0 < \log(t) < 7.4$; and old (o): $7.5 < \log(t) < 8.2$. As discussed in Section 3.2.3, NGC 1850 likely contains populations of multiple epochs, thus we assign it a designation of “old” with caution.

Table 6: Average Number of Early- and Later-Type Candidate Be Stars in Every Cluster

Cluster	Age	Location	Early-Type	Later-Type
NGC 371	vy	SMC	86/736 (12% ± 1%)	43/348 (12% ± 2%)
NGC 346 ²	vy	SMC	11/78 (14% ± 4%)	...
LH 72	vy	LMC	28/158 (18% ± 3%)	15/75 (20% ± 5%)
NGC 1858	vy	LMC	33/95 (35% ± 5%)	...
NGC 1955	vy	LMC	9/96 (9% ± 3%)	13/41 (32% ± 7%)
NGC 330 ²	y	SMC	27/79 (34% ± 5%)	...
NGC 330 ¹	y	SMC	50/128 (39% ± 4%)	...
NGC 456	y	SMC	20/58 (34% ± 6%)	1/28 (4% ± 4%)
NGC 460	y	SMC	16/73 (22% ± 5%)	5/20 (25% ± 10%)
NGC 2006 ¹	y	LMC	10/35 (29% ± 8%)	...
NGC 2004 ¹	y	LMC	25/130 (19% ± 3%)	...
NGC 2027	y	LMC	32/329 (10% ± 2%)	7/219 (3% ± 1%)
Hodge 301 ¹	y	LMC	10/44 (23% ± 6%)	...
NGC 1818A ¹	y	LMC	34/94 (36% ± 5%)	...
NGC 1948 ¹	y	LMC	11/101 (11% ± 3%)	...
NGC 2100 ¹	y	LMC	19/67 (28% ± 6%)	...
NGC 1818 ²	y	LMC	19/92 (21% ± 4%)	...
NGC 2004 ²	y	LMC	16/124 (13% ± 3%)	...
SL 538 ¹	y	LMC	11/46 (24% ± 6%)	...
NGC 457 ¹	y	MW ext.	4/28 (14% ± 6%)	...
NGC 663 ¹	y	MW ext.	12/35 (34% ± 8%)	...
NGC 869 ¹	y	MW ext.	3/42 (7% ± 4%)	...
NGC 884 ¹	y	MW ext.	6/28 (21% ± 8%)	...
NGC 2439 ¹	y	MW ext.	5/31 (16% ± 6%)	...
NGC 3293 ¹	y	MW int.	1/37 (3% ± 3%)	...
NGC 3766 ¹	y	MW int.	10/42 (24% ± 7%)	...
NGC 4755 ¹	y	MW int.	3/47 (6% ± 3%)	...
Bruck 60	o	SMC	22/73 (30% ± 5%)	4/25 (16% ± 7%)
NGC 458	o	SMC	5/21 (24% ± 10%)	10/39 (26% ± 7%)
NGC 1850	o?	LMC	56/350 (16% ± 2%)	36/142 (25% ± 4%)

Note. — The superscript “1” denotes data culled from Maeder, Grebel, & Mermilliod (1999) while the superscript “2” denotes data culled from Keller et al. (1999). All of the cluster data taken from the literature correspond to “young” clusters (Maeder, Grebel, & Mermilliod 1999), although we note that age estimates differing by up to a factor of 2 from those listed in Maeder, Grebel, & Mermilliod (1999) may be found elsewhere in the literature.

Table 7: Number of Early- and Later-Type Candidate Be Stars Averaged by Common Metallicity Environment

Region	Age	Early-Type	Size	Later-Type	Size
SMC	vy	$13\% \pm 3\%$	2	$12\% \pm 2\%$	1
LMC	vy	$20\% \pm 4\%$	3	$26\% \pm 6\%$	2
SMC	y	$32\% \pm 5\%$	4	$15\% \pm 8\%$	2
LMC	y	$21\% \pm 5\%$	10	$3\% \pm 1\%$	1
MW ext.	y	$18\% \pm 7\%$	5
MW int.	y	$11\% \pm 5\%$	3
SMC	o	$27\% \pm 8\%$	2	$21\% \pm 7\%$	2
LMC	o	$16\% \pm 2\%$	1	$25\% \pm 4\%$	1

Note. — The fractional Be content of clusters having similar ages and metallicities in Table 6 were averaged to produce the data in this table. Clusters with fewer than 20 objects in a spectral bin were not used in the averaging procedure. The column labeled size corresponds to the sample size of clusters used to compute these averages.

Table 8: Main Sequence Lifetimes of Early B-Type Stars

Mass	Initial Rot. Velocity	Mid-MS Lifetime	Mid-MS Lifetime	MS Lifetime	MS Lifetime
		SMC	Solar	SMC	Solar
25 M_{sun} (\sim O9)	0	3.6 Myr	3.0 Myr	7.2 Myr	5.9 Myr
...	300 km s ⁻¹	3.9 Myr	3.7 Myr	7.8 Myr	7.4 Myr
15 M_{sun} (\sim B0)	0	6.1 Myr	5.1 Myr	12.2 Myr	10.2 Myr
...	300 km s ⁻¹	6.8 Myr	6.5 Myr	13.6 Myr	12.9 Myr
12 M_{sun} (\sim B1)	0	8.3 Myr	7.0 Myr	16.6 Myr	13.9 Myr
...	300 km s ⁻¹	9.3 Myr	8.4 Myr	18.6 Myr	16.8 Myr
9 M_{sun} (\sim B2)	0	13.0 Myr	11.1 Myr	25.9 Myr	22.1 Myr
...	300 km s ⁻¹	14.7 Myr	13.4 Myr	29.3 Myr	26.7 Myr

Note. — The mid-point main sequence lifetimes and main sequence lifetimes of rotating and non-rotating stars in solar and low metallicity environments is tabulated, as calculated by Meynet & Maeder (2000) and Maeder & Meynet (2001). The general spectral types associated with each entry were based upon the masses of individual spectral types given by Landolt-Bornstein (1982): O9 = 23 M_{sun} , B0 = 17.5 M_{sun} , B1 = 13 M_{sun} , B2 = 7.6 M_{sun} , and B3 = 5.9 M_{sun} .

Table 9: Spectral Types of Candidate Be Stars in Galactic Clusters

Cluster	B0	B1	B2	B3	B4	B5	B6	B7	B8
NGC 2186	0/0	1/1	0/0	0/0	2/2	0/0	1/1	1/1	0/0
NGC 2439	3/8	1/7	0/14	0/4	0/10	0/18	0/22	1/11	0/19

Note. — Spectral types were assigned using the calibrations of Zorec & Briot (1997), following the methods outlined by Grebel (1997): $B_0 : M_V < -3.25$, $B_1 : -3.25 < M_V < -2.55$, $B_2 : -2.55 < M_V < -1.8$, $B_3 : -1.8 < M_V < -1.4$, $B_4 : -1.4 < M_V < -0.95$, $B_5 : -0.95 < M_V < -0.6$, $B_6 : -0.6 < M_V < -0.25$, $B_7 : -0.25 < M_V < 0.025$, $B_8 : 0.025 < M_V < 0.285$. For the purposes of this Table, we have increased the observed m_V for our NGC 2186 data by 1.0 magnitudes to correct for the systematic errors known to reside in these data (see Sections 2 and 3.3.1 for further details regarding these errors).